CLONING AND STEM CELLS
Volume 8, Number 3, 2006

Human Embryonic Stem Cell–Derived Cells Rescue Visual Function in Dystrophic RCS Rats

RAYMOND D. LUND,[1] SHAOMEI WANG,[1] IRINA KLIMANSKAYA,[2] TOBY HOLMES,[1] REBECA RAMOS-KELSEY,[2] BIN LU,[1] SERGEJ GIRMAN,[1] N. BISCHOFF,[1] YVES SAUVÉ,[3] and ROBERT LANZA[2]

ABSTRACT

Embryonic stem cells promise to provide a well-characterized and reproducible source of replacement tissue for human clinical studies. An early potential application of this technology is the use of retinal pigment epithelium (RPE) for the treatment of retinal degenerative diseases such as macular degeneration. Here we show the reproducible generation of RPE (67 passageable cultures established from 18 different hES cell lines); batches of RPE derived from NIH-approved hES cells (H9) were tested and shown capable of extensive photoreceptor rescue in an animal model of retinal disease, the Royal College of Surgeons (RCS) rat, in which photoreceptor loss is caused by a defect in the adjacent retinal pigment epithelium. Improvement in visual performance was 100% over untreated controls (spatial acuity was approximately 70% that of normal nondystrophic rats) without evidence of untoward pathology. The use of somatic cell nuclear transfer (SCNT) and/or the creation of banks of reduced complexity human leucocyte antigen (HLA) hES-RPE lines could minimize or eliminate the need for immunosuppressive drugs and/or immunomodulatory protocols.

INTRODUCTION

HUMAN STEM CELL DERIVATIVES have been considered a promising source of tissue for regenerative medicine (Banin et al., 2006; Correia et al., 2005; Dunnett and Rosser, 2004; Haruta, 2005; Lanza et al., 2004; Mueller et al., 2005). The ability to generate GMP-grade retinal pigment epithelium (RPE) from human embryonic stem (hES) cells under well-defined and reproducible conditions would provide a scalable and efficacious product for use in human conditions such as age-related macular degeneration (ARMD) where photoreceptor loss is resultant upon RPE dysfunction. ARMD alone affects more than 30 million people worldwide and is the leading cause of blindness in patients over 60 in the United States (Friedman et al., 2004). Previous work has shown that freshly harvested RPE can be effective in rescuing photoreceptors in the Royal College of Surgeons (RCS) rat, an animal model of indirect photoreceptor degeneration, the RCS rat (Li et al., 1996; Sheedlo et al., 1991). In this animal, a mutation in the MERTK gene affects the ability of RPE cells to phagocytose photoreceptor outer segments (D'Cruz et al., 2000) and leads to loss of photoreceptors over a several month time frame (LaVail, 2001). There is a small group of humans who have been identified with orthologous mutations (Gal et al., 2000; Tada et al., 2006), but the main value of the animal has been its extensive use in exploring conditions under which photoreceptors can be rescued.

[1]Moran Eye Center, University of Utah Health Science Center, Salt Lake City, Utah.
[2]Advanced Cell Technology, Worcester, Massachusetts.
[3]Ophthalmology and Physiology, University of Alberta, Edmonton, Canada T6G.

A major issue in any cell-based therapy is that of providing a cell source that is readily available, safe, and ethically acceptable and which can be developed commercially in large-scale production. With this goal in mind, we recently reported the isolation of RPE cells from hES cells which could be maintained through multiple passages (>30 population doublings) (Klimanskaya et al., 2004). Gene expression profiling demonstrated their higher similarity to primary RPE tissue than of existing human RPE cell lines D407 and the spontaneously generated ARPE19 line. Here we show that new RPE can be re-established in a reliable and reproducible manner from 18 different hES lines. We have studied one of these lines to show using morphological, behavioral and physiological techniques that these cells have the capacity to support photoreceptor survival and preserve visual function after subretinal transplantation into RCS rats. The cells did not undergo tumorous transformation after long-term transplantation nor did they provoke overt pathological responses in the host retina.

METHODS

Human embryonic stem cell lines

The hES cell lines used in this study were previously described H1, H7, and H9 (Thomson et al., 1998) (National Institutes of Health–registered as WA01, WA07, and WA09), and 15 lines derived with the use of private funds (eight of these lines were derived at Harvard University in the laboratory of Douglas Melton (Cowan et al., 2004), and seven were derived at Advanced Cell Technology). The later 15 hES cell lines were derived from human frozen blastocysts or cleaved embryos that were donated by couples who had completed their fertility treatment. hES cells were maintained on mitomycin C-treated mouse embryonic fibroblasts (MEF) in growth medium: knockout high glucose DMEM supplemented with 500 μ/mL penicillin, 500 μg/mL streptomycin, 1% non-essential aminoacids solution, 2 mM GlutaMAX I, 0.1 mM β-mercaptoethanol, 4 ng/mL bFGF (Invitrogen), 1-ng/mL human LIF (Chemicon, Temecula, CA), 8% of Serum Replacement (SR, Invitrogen), and 8% Plasmanate (Bayer). The cells were routinely passaged with trypsin at a ratio of 1:3–1:6 every 3–5 days (Klimanskaya and McMahon, 2004).

Cell isolation and characterization

hES were cultured as described above and allowed to spontaneously differentiate: this resulted in the appearance of RPE clusters over the course of 6–8 weeks, from which hES-RPE cells were isolated and subcultured (Klimanskaya et al., 2004). Spontaneous differentiation was observed in 7–10-day-old cultures, and the cells were switched to differentiation medium containing 15% SR in knockout high glucose DMEM supplemented with 500 μ/ml penicillin, 500 μg/mL streptomycin, 1% non-essential aminoacids solution, 2 mM GlutaMAX I, 0.1 mM β-mercaptoethanol, 4 ng/mL bFGF (Invitrogen), 10 ng/mL human LIF (Chemicon), The first pigmented clusters were usually observed in 6–8 weeks after the initial plating of hES cells, and the cells were isolated by hand-picking under the microscope after such clusters reached the desired size and number. Isolated cells were subcultured in knockout high glucose DMEM supplemented with 500 μ/mL penicillin, 500 μg/mL streptomycin, 1% non-essential aminoacids solution, 2 mM GlutaMAX I, 0.1 mM β-mercaptoethanol, 7% SR, 5% FBS on gelatin. The cells were subcultured with 0.25% Trypsin/1 mM EDTA (Invitrogen) and passaged at 1:3 ratio after the cells re-established the RPE phenotype, usually 2–3 weeks after passaging.

Cell injections

hES-RPE derived from hES cell line WA09 were passaged three or four times and pooled together prior to injection. An aliquot of the final cell suspension was frozen and later analyzed by RT-PCR and real-time PCR. At P21–23, 14 dystrophic RCS rats under xylazine-ketamine anesthesia received subretinal injections of a suspension of cells (2×10^4cells/eye) via a trans-scleral approach into the upper temporal retina area as previously described (Wang et al., 2005). As control material, some rats ($n = 8$) received an injection of medium alone. Dystrophic rats that had received injections of the RPE cell line, ARPE-19 (American Type Culture Collection [ATTC], Manassas, VA), and non-dystrophic congenic rats were available for comparison. All animals received daily dexamethasone injections (1.6 mg/kg, i.p.) for 2 weeks and were maintained on cyclosporine-A (Bedford Labs, Bedford MA) administered in the drinking water (210 mg/L; resulting blood concentration: 250–300 μg/L) (Prusky et al., 2004) from 1–2 days prior to cell injection until animals were euthanized.

Electroretinogram responses

The dark adapted electroretinogram (ERG) response was recorded as previously described (Pinilla et al., 2004). A double flash protocol was used to isolate cone responses. A conditioning flash was followed 1 sec later by a probe flash. The role of the conditioning flash in this paradigm is to saturate rods transiently so that they are rendered unresponsive to the probe flash. The intensity of the conditioning flash for complete rod bleaching was set to 1.4 log cd / m^2 for all tests. A mixed b-wave was obtained by presenting the probe flash alone, i.e., without being preceded by a conditioning flash. The response to the probe flash (1.4 log cd / m^2), preceded by the conditioning flash, was taken as reflecting cone-driven activity, and allowed derivation of the rod contribution. Averages of 3–5 traces (set at 2 min apart to assure recovery of rod responsiveness) were sufficient to obtain clear responses. Special care was taken to maintain the electrode placement in a consistent position in all animals.

Optomotor acuity thresholds

Thresholds to moving stripes of varying spatial frequency were measured at P90–100. An image of a rotating cylinder covered with a vertical sine wave grating was presented in virtual three-dimensional (3D) space on four computer monitors arranged in a square (Douglas et al., 2005; Prusky et al., 2004). Rats standing unrestrained on a platform in the center of the square tracked the grating with reflexive head movements. The spatial frequency of the grating was clamped at the viewing position by repeatedly recentering the "cylinder" on the head of the test subject. Acuity threshold was quantified by increasing the spatial frequency of the grating until an optomotor response could no longer be elicited. The method, a development of a rotating drum with fixed stripes, has several distinct advantages over the older technology, most important of which are that individual animals show less variance between trials, it allows tighter titration of acuity, and it is quicker to perform so animals do not become distracted or go to sleep during testing.

Luminance threshold recording

After optomotor testing, luminance thresholds were established in selected rats ($n = 7$) by recording single and multiunit activity in the superficial layers of the SC using a modification of a procedure we developed in previous work (Sauve et al., 2002). For each of 16–20 positions recorded over the surface of the SC, a discrete receptive field for that position was localized and the brightness of a flashing spot, 3-degrees-diameter projected on a hemisphere, was varied with neutral density filters until a response amplitude was diminished to a level double that of background activity.

Histology

Rats were overdosed with sodium pentobarbital (Sigma, St. Louis, MO) and perfused with phosphate-buffered saline (PBS). The eyes were removed and immersed in 2% paraformaldehyde for 1 h, infiltrated with sucrose and embedded in OCT. Coronal sections (10 μm) were cut on a cryostat. Five 1-in-5 series were collected. One series was stained with Cresyl violet (CV) for assessing injection site, retinal lamination, and evidence of cellular infiltrates or tumor formation. Further series were stained with human-specific nuclear marker—MAB1281 (Chemicon)—for donor cells; PCNA for dividing cells and RPE65; bestrophin for RPE cells; and recoverin (a gift from Dr. J. McGinnis, University of Oklahoma) for photoreceptors. The protocols for processing human-specific nuclear marker followed the manufacturers' data sheets. The secondary antibodies were biotinylated anti-mouse or rabbit IgG or conjugated with FITC or Cy3 (Jackson). The cells were visualized by using Vector Nova RED (Vector Labs, Burlingham, CA) for human nuclear marker. Photographs were taken by using the Image-pro-Plus program; montage pictures were achieved using Photoshop. For confocal images, the pinholes were 75 μm and the width of optical sections was 1 μm. Final images were obtained from the projections of 6–8 single frames. The TIFF images were produced in Adobe Photoshop.

RNA extraction and RT-PCR

Total RNA from the RPE cells was isolated by using RNeasy Mini Kit (Qiagen) with the on-column DNAase treatment. Gene-specific primer pairs were designed for the following genes:

RPE65-F: ATGGACTTGGCTTGAATCACTT,
RPE65-R: GAACAGTCCATGAAAGGTGACA
Bestrophin-F: TAGAACCATCAGCGCCGTC

Table 1. Reproducible Generation of Retinal Pigment Epithelium (RPE) Lines from Human Embryonic Stem (ES) Cells

	Passage no.	*No. RPE lines established*
ES cell line		
WA01 (H1)	30–126	15
WA09 (H9)	44–67	7
WA07 (H7)	25	1
Total H lines		23
MA01	6, 9	2
MA03	5–10	4
MA04	5–27	5
MA09	7	1
MA14	13	1
MA40	5–27	8
MAJ1	3–17	5
Total MA lines		26
HUES1	25–43	5
HUES2	30–36	2
HUES3	15–28	3
HUES5	8	1
HUES6	8–12	2
HUES7	7–14	2
HUES8	7–14	2
HUES10	8	1
Total HUES lines		18
Total no. RPE lines isolated		67

Bestrophin-R: TGAGTGTAGTGTGTATGTTGG
CRALBP-F: AAATCAATGGCTTCTGCATCATT
CRALBP-R: CCAAAGAGCTGCTCAGCAAC
PEDF-F: TCTCGGTGTGGCGCACTTCA
PEDF-R: GTCTTCAGTTCTCGGTCTATG
GADPH-F: CGATGCTGGCGCTGAGTAC
GADPH-R: CCACCACTGACACGTTGGC

Reverse transcription–polymerase chain reaction (RT-PCR) was performed with 0.5–1 μL of RNA by using a OneStep RT-PCR Kit (Qiagen) with the addition of 10 units of RNasin Ribonuclease Inhibitor (Promega) under the following conditions in a GeneAmp Perkin Elmer thermocycler: cDNA synthesis 50°C, 30 minutes; DNA polymerase activation 95°C, 15 min; 35 cycles of denaturation 94°C, 30 sec; annealing 55°C, 30 sec; extension 72°C, 1 min; final extension 72°C, 10 min. For negative control, total RNA was excluded from the reaction mixture and RNase-free water was used instead. PCR products were separated on a 1.5% agarose gel stained with 0.5 mg of ethidium bromide for 30 min, and the fluorescence was scanned using a Kodak Image Station 4000MM.

Statistical analysis

Average data are presented as mean ± SEM (or mean ± SD). We used *t*-test or Mann-Whitney *U* for comparisons unless otherwise indicated (Statview). Significance is designated as $p < 0.05$.

RESULTS

Generation of RPE cell lines

All 18 hES cell lines studied reliably produced passageable RPE lines after 6–8 weeks of spontaneous or induced differentiation (Table 1). The differentiation system did not require co-culture with animal cells or factors as previously described (Haruta et al., 2004). Multiple RPE clusters appeared in adherent cultures and in embryoid bodies (EB), and were used to establish 67 repeatedly passageable (>5 passages) RPE lines with RPE features, such as phenotype and the ability to transdifferentiate and differentiate thorough multiple passages. Figure 1 shows expression of RPE molecular markers in representative samples of hES-derived RPE lines compared to human fetal RPE cells. Reverse transcription–polymerase chain reaction (RT-PCR) detected the presence of RPE65, bestrophin, and PEDF in all samples analyzed (Fig. 1A–E).

The appearance and characterization of the hES-derived RPE cell line used in the animal studies is shown in Figure 2. Differentiation of

FIG. 1. Molecular marker analysis of human embryonic stem cell (hES)–derived retinal pigment epithelium (RPE) lines. (**A-C**) Reverse transcription–polymerase chain reaction (panels are composites of gel images from several representative experiments). (**D,E**) Immunofluorescence. (**A**) Bestrophin: 1—C2C12 cells (negative control); 2—fetal RPE (positive control); 3—MA03; 4—MA40; 5—WA01; 6—WA09; 7—MAJ1. (**B**) PEDF: 1—C2C12 cells (negative control); 2—fetal RPE (positive control); 3—MA03; 4—MA40; 5—MA09; 6—WA01; 7—WA09; 8—MAJ1. (**C**) RPE65: 1—C2C12 cells (negative control); 2—fetal RPE (positive control); 3—MA03; 4—MA40; 5—MA09; 6—WA01; 7—WA09. (**D**) Culture of hES-RPE cells, Hoffman modulation optics. (**E**) Same field stained with antibodies to bestrophin. Scale bar = 100 μm.

FIG. 2. Human embryonic stem cell (hES0)–derived retinal pigment epithelium (RPE) used for injection. (**a**) Hoffman modulation optics micrograph of cells 12 days after passaging. Note that the cells are in the process of re-established pigmented phenotype. Scale bar = 100 μm. (**b**) Expression of RPE molecular markers detected by reverse transcription–polymerase chain reaction (RT-PCR): 1—hES-RPE; 2—fetal RPE; 3—negative control (no template). (Panel is a composite of gel images from several representative experiments.)

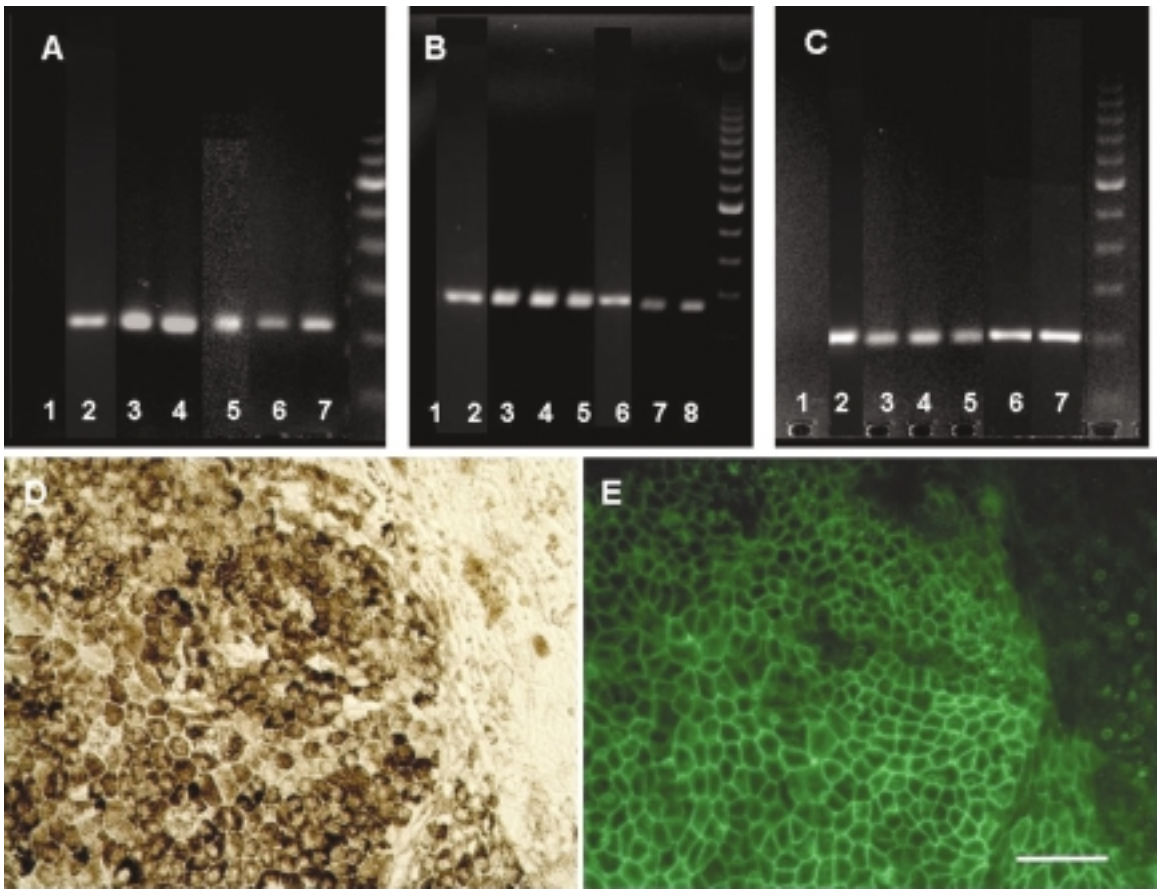
A
1 2 3 4 5 6 7
B
1 2 3 4 5 6 7 8
C
1 2 3 4 5 6 7
D
E

FIG. 1.

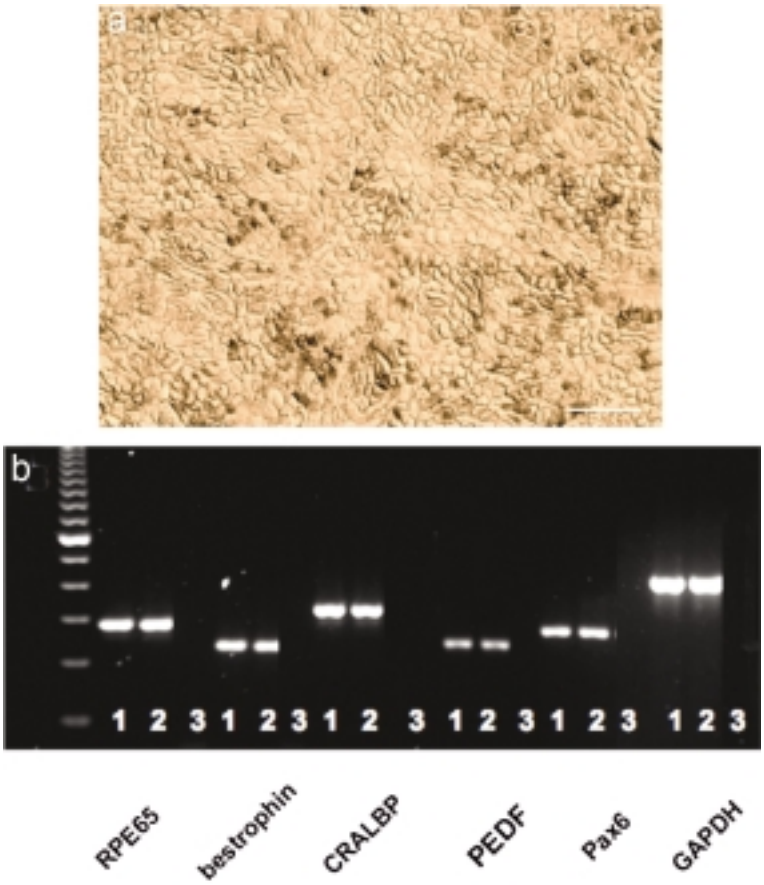
a
b
1 2 3 1 2 3 1 2 3 1 2 3 1 2 3 1 2 3
RPE65
bestrophin
CRALBP
PEDF
Pax6
GAPDH

FIG. 2.

hES cell line WA09 (H9) was induced at passages 65–66, and hES-RPE were subcultured for several passages prior to transplantation and examining *in vivo* efficacy. Passaging was performed after the cells went through the transdifferentiation–differentiation cycle and re-established a mature RPE phenotype, including typical RPE "cobblestone" morphology (Fig. 2a). Real-time RT-PCR assessment of the cells was carried out at the time of transplantation and compared to primary human fetal RPE tissue. Both hES-RPE and fetal RPE displayed high expression of characteristic RPE genes, including RPE65, bestrophin, CRALBP, and PEDF (Fig. 2b).

Efficacy of cell line WA09 (H9) after transplantation to RCS rat eyes

Eye-pigmented RCS rats received injections of hES-RPE into the subretinal space of the eye between the RPE and photoreceptor layers at postnatal day (P) 21 at an age when photoreceptor degeneration had yet to develop.

Electroretinogram (ERG) responses were tested at both P60 and P90 to measure the electrical activity of the outer (a-wave) and inner (b-wave) retina to light flashes. Double flash presentations allowed isolation of rod and cone-related activity, respectively. At P60, the a-wave ERG response is normally lost in RCS rats, and by P90, the b-wave response is severely depleted, allowing graft-related effects to be recognized over background performance (Pinilla et al., 2005b). By P60, the hES-RPE-grafted animals achieved significantly better a-wave, b-wave, and cone mediated responses over untreated and sham-injected animals (Fig. 3A). As with other studies using ARPE-19 cells (Pinilla et al., 2004, 2005a), there was deterioration of the magnitude of the responses by P90, but other tests showed continued robust visual performance. One of these was an optomotor test that provided a measure of spatial acuity (Douglas et al., 2005; Prusky et al., 2004). Normal non-dystrophic rats gave a figure of approximately 0.6 cycles / degree (c / d), while in sham-injected rats, a threshold response of 0.29 ± 0.03 c / d was recorded at P100: untreated animals gave a figure of 0.21 ± 0.03 c / d. By contrast, the cell-grafted rats sustained levels of 0.42 ± 0.03 c / d, significantly better than sham-injected rats ($p < 0.05$, *t*-test). The best animals performed at 0.45 c / d (Fig. 3B).

Animals from each group were selected for testing luminance threshold responses. We chose both average and best performers in the optomotor test for such assessment. The minimum light intensity that could elicit neuron activation at various points across the visual field representation was measured by recording unit activity from different locations across the superior colliculus (SC). To reduce the data for ease of presentation and statistical analysis, however, it is presented here as the percentage of the collicular area (*y*-axis) from which the responses showed visual thresholds less than the value designated on the *x*-axis (log units over a background illumination of 0.02 log candela / m^2). Asterisks indicate the points at which the curves for grafted and sham-operated eyes were statistically different (*t*-test, $p < 0.05$). Results were obtained from animals receiving hES-RPE cells ($n = 7$), sham injections ($n = 5$), and no treatment ($n = 6$). In non-dystrophic rats, a threshold response of less than 0.6 log units is recorded. As can be seen in Figure 3C, by P 100, neurons across the whole visual field failed to respond with thresholds of 2.7 log units or better in an untreated dystrophic RCS rat, while responses could be elicited from 18% of the area in sham-injected rats. By comparison, the cell-injected rats showed 52% of the collicular area with thresholds of 2.7 log units or better, with a best point of 1.3 log units.

Anatomical examination of the retinas showed that donor hES-RPE cells, identified using human specific nuclear marker, were distributed in the subretinal space adjacent to the host RPE layer (Fig. 4d). Two RPE-specific markers—RPE65 and bestrophin—stained these cells positively. Human-specific proliferating cell nuclear antigen (PCNA) staining was negative, indicating lack of continued cell division among the donor cells. There was extensive photoreceptor rescue: 5–7 cells deep in the outer nuclear layer (ONL; Fig. 4a,b). For comparison, the ONL was 10–12 cells deep in nondystrophic rats, while in dystrophic rats, this layer was reduced to one cell deep at P100 (Fig. 4c). Sham injected retinas appeared similar to unoperated dystrophic rats except for a small cluster of remaining photoreceptors immediately adjacent to the injection site and a comparable appearance was seen in graft-protected retinas distant from the area of distribution of grafted cells. Antibody staining against recoverin confirmed the presence of a well-preserved photoreceptor layer with inner and outer segments evident in the graft-protected area, while distant

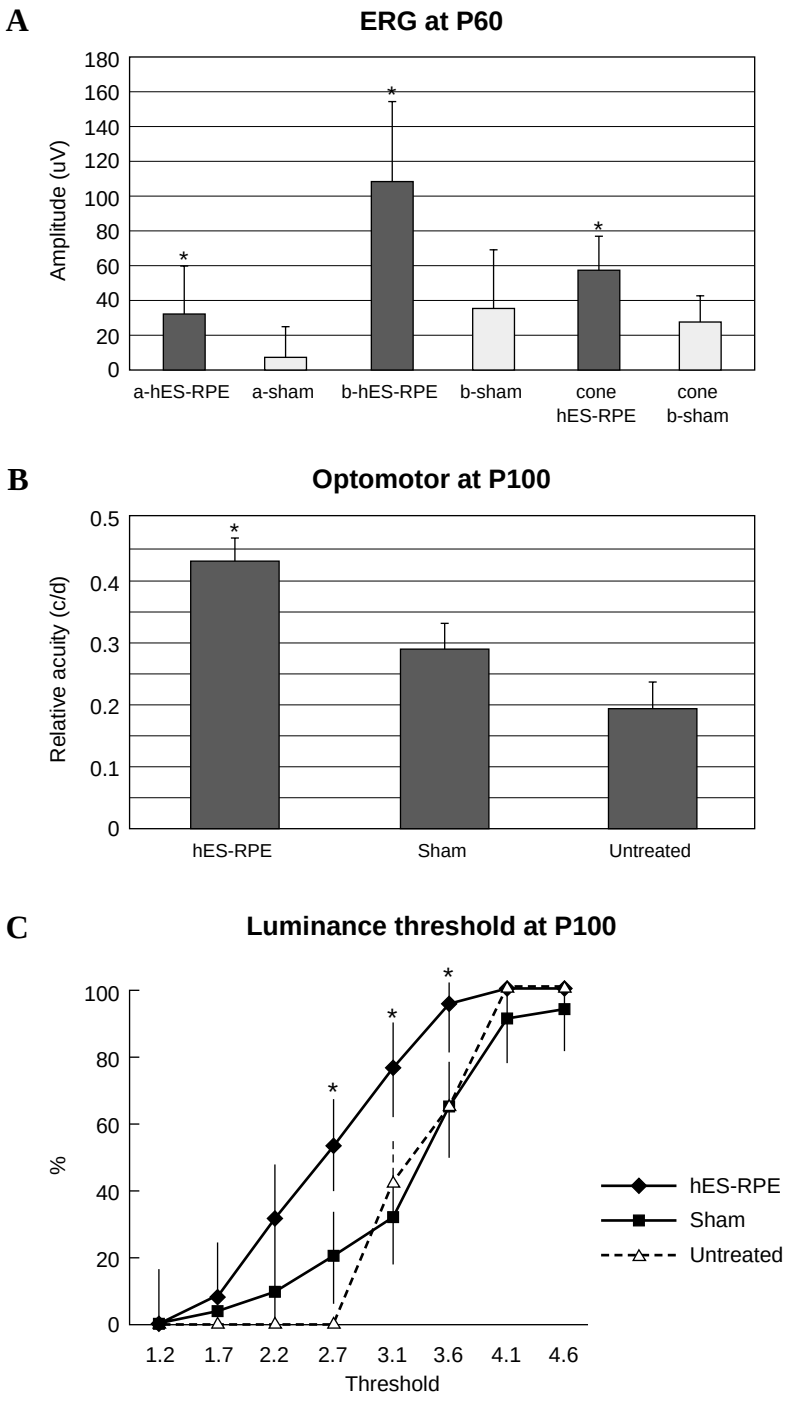

FIG. 3. Functional assessment of human embryonic stem cell (hES)–derived retinal pigment epithelium (RPE) after subretinal transplantation in Royal College of Surgeons (RCS) rats. (**A**) hES-RPE grafted animals achieved significantly better responses over sham controls ($p < 0.05$, *t*-test) for a-wave (31 ± 27 vs. 6 ± 17 μV), b-wave (108 ± 46 μV vs. 36 ± 33 μV) and cone b-wave (57 ± 19 vs. 28 ± 13 μV). (**B**) The relative acuity as measured by the optomotor system shows that the hES-RPE treated eyes perform significantly better than the medium treated and untreated eyes ($p < 0.05$, *t*-test), giving approximately 50% and 100% improvement in visual acuity over the sham and untreated controls, respectively. Non-dystrophic untreated eyes give readings of 0.53–0.6 cycles / degree (**c/d**). (**C**) Luminance threshold responses recorded across the superior colliculus, each curve (average $\pm$ SEM) shows the percent of retinal area (*y*-axis) where the visual threshold is less than the corresponding value on the *x*-axis (log units, relative to background illumination 0.02 cd / m^2). Asterisks show the points where the curves for grafted and sham-operated eyes are statistically different (*t*-test, $p < 0.05$). The curves show that 52% of the area of the superior colliculus (SC) in grafted animals gave thresholds of 2.7 log units and against shams in which approximately 18% gave thresholds of 2.7 log units.

from graft, sparsely distributed photoreceptors remained (Fig. 4e,f). There was no indication of extraneous cells in the retina, particularly in the plexiform layers where invasive cells can be easily recognized even in Cresyl violet–stained sections. None of the retinas showed evidence of uncontrolled cell proliferation, including tumor formation.

DISCUSSION

Our results show that a well-characterized derivative of human embryonic stem cells—retinal pigment epithelium (RPE)—is capable of significant rescue of visual function in a clinically relevant animal model of retinal disease. The cells survived long-term (>100 days) after transplantation into RCS rats, and localized to the subretinal space without migration into the retina. In addition to extensive photoreceptor rescue (5–7 cells deep in the outer nuclear layer), the relative acuity as measured by the optomotor system showed that animals treated with hES-derived RPE performed significantly better than sham and untreated controls (50% and 100% improvement in visual performance, respectively; visual acuity was approximately 70% that of normal non-dystrophic rats). However, the broader role of hES-derived cells in taking on the full range of RPE cell functions beyond photoreceptor rescue still remains to be explored *in vivo*.

Detailed quantitation of rescue was limited to functional measures based on previous work in RCS rats. Although rods can be rescued by at least two very different cell transplants, they do not function normally, if at all, but rather deterioration of cone-meditated vision was limited (Girman et al., 2005). Therefore, counting cells on the ONL, comprising 97% rods, gives at best an indirect measure of the degree of vision sustained. Rescue is in the same order as that achieved previously using ARPE-19 cells (Lund et al., 2001) and other cells that appear to function by delivery of growth factors (Wang et al., 2005; Lawrence et al., 2004). However, apart from having a molecular profile more closely resembling native RPE than do ARPE-19 cells (Klimanskaya et al., 2004), the present cells afford certain advantages over ARPE-19 in that many lines can be generated. Given the immunoprovocative nature of RPE cells, the use of hES cells would allow opportunity to generate appropriate immunogenetic lines using various HLA-matching strategies. While rescue can be achieved by growth factor delivery either by cell-based approaches such as using Schwann cells (Wang et al., 2005) or cells transfected to deliver specific growth factors (Lawrence et al., 2004) as well as by direct injection (LaVail et al., 1992), this approach is unlikely to replace all the functions of RPE cells. Since the present cells closely resemble RPE cells (Klimanskaya et al., 2004), they are more likely to replicate a broader range of RPE functions than ARPE-19 or by simple factor delivery. The aim here was to demonstrate that the cells remain localized in the subretinal space and can support photoreceptor survival as well as a range of visual functions.

There are numerous advantages of using hES-derived cells as a source of RPE for clinical studies. Primary RPE tissue cannot be obtained in large enough quantities for wide-scale clinical use. Furthermore, practical restrictions prevent full safety testing from being performed on every fetal or adult donor source, nor can the functional parameters of graft efficacy be systematically assessed. In contrast, hES-RPE can be derived and maintained under well-defined and reproducible conditions using traceable reagents, including specific lots of media, sera, growth factors, and other culture materials. New and additional banks of RPE can be created to test and further optimize yields and functionality. RPE differentiation appears to be an inevitable event in hES cultures, and we have obtained consistent differentiation of human ES cells to RPE, including long-term hES cul-

FIG. 4. Anatomical rescue of photoreceptors after transplantation of human embryonic stem cell (hES)–derived retinal pigment epithelium (RPE). (**a–c**) Retinal sections at P100 stained with cresyl violet: extensive photoreceptor rescue with hES-RPE graft (**a**); high-power image of the rescued outer nuclear layer (ONL), which is 5–7 cells deep (**b**); distant from graft, the ONL is reduced to a single layer (**c**). (**d**) grafted retina section stained with human nuclear marker (arrows indicate positively stained donor cells). (**e,f**) Confocal microscopic images of retinal sections double stained with recoverin (green) and PKCa (red): graft protected area (**e**) had several layers of ONL with inner segments, rod bipolar cells have denser terminals, whereas at area distant from graft (**f**), there is only a single layer of ONL, and the rod bipolar cell terminals are reduced in density. Scale bar = 200 μm (**a**), 20 μm (**b–f**).

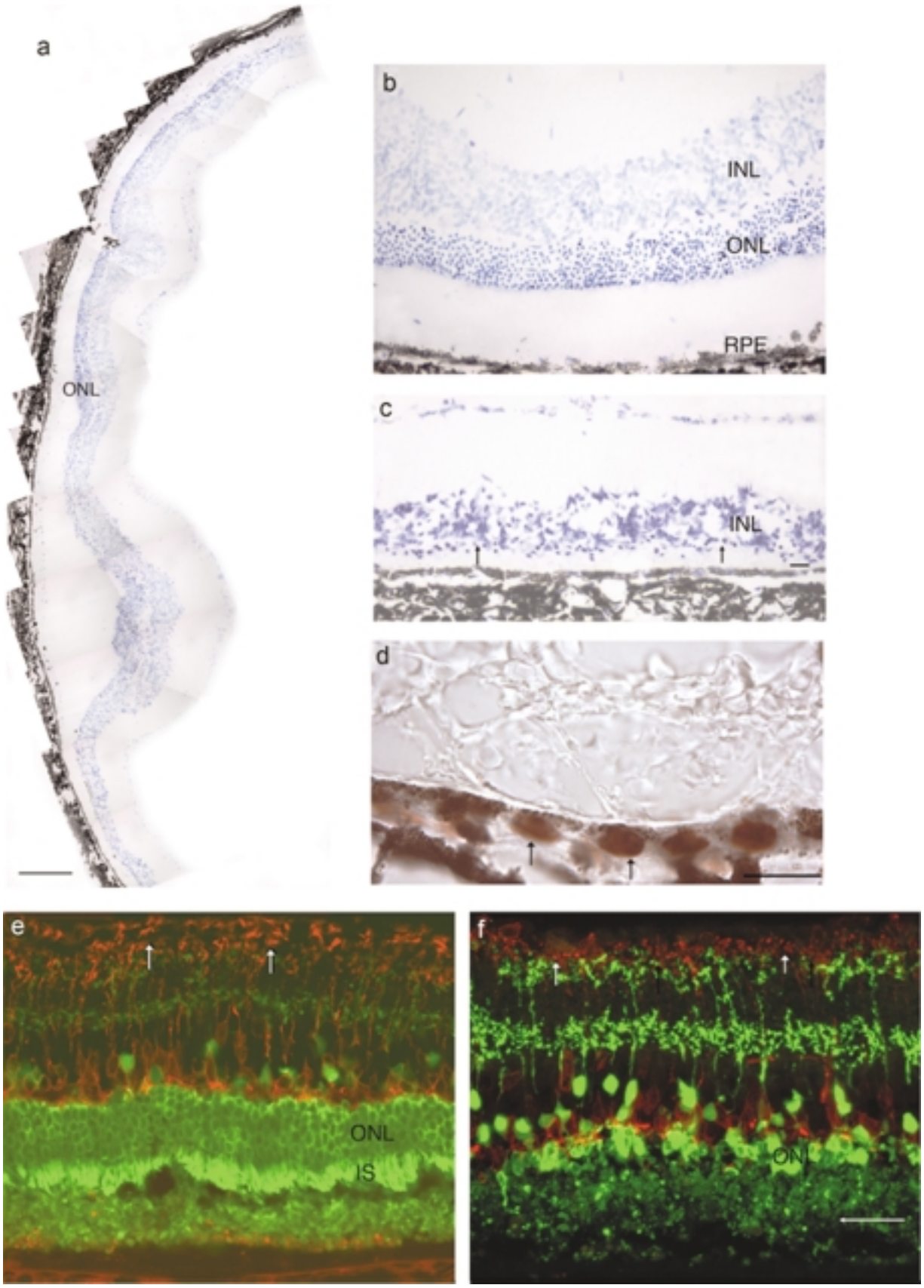
a
ONL
b
INL
ONL
RPE
c
INL
d
e
ONL
IS
f
ONL

tures grown either on feeder layers or feeder-free on gelatin, fibronectin, laminin, collagen type I and IV, or in EBs. Importantly, there also remains the issue of immunogenicity. It has been found that despite the immunoprivileged status of the eye, allogeneic RPE cells can still be rejected, albeit less floridly than a typical tissue mismatch allograft (Zhang and Bok, 1998). With the further development of somatic cell nuclear transfer (SCNT), parthenogenesis, or the creation of banks of reduced-complexity human leucocyte antigen (HLA) hES cells, RPE lines could be generated to overcome the problem of immune rejection and the need for immunoprotective regimens.

ACKNOWLEDGMENTS

We would like to acknowledge the excellent technical support provided by Tong Lin (ACT), and Elena Budko and Jennifer Hunter (Moran Eye Center). The R.D.L. laboratory was supported by grants from the Foundation Fighting Blindness and the Wynn Foundation. R.D.L. is a recipient of a Research to Prevent Blindness Senior Scientific Investigator Award. Work with the HUES lines was initiated at Harvard University in the laboratory of Douglas Melton with support from the Howard Hughes Medical Institution (HHMI) and the Juvenile Diabetes Research Foundation (JDRF).

DISCLOSURE

I.K., R.K., and R.P. are employees of Advanced Cell Technology, a stem cell company in the field of regenerative medicine. R.D.L., S.W., T.H., B.L., S.G., N.B., and Y.S. declare that they have no competing financial interests.

REFERENCES

Banin, E., Obolensky, A., Idelson, M., et al. (2006). Retinal incorporation and differentiation of neural precursors derived from human embryonic stem cells. Stem Cells 24, 246–257.

Correia, A.S., Anisimov, S.V., Li, J.Y. et al. (2005). Stem cell–based therapy for Parkinson's disease. Ann. Med. 37, 487–498.

Cowan, C.A., Klimanskaya, I., McMahon, J., et al. (2004). Derivation of embryonic stem cell lines from human blastocysts. N. Engl. J. Med. 350, 1353–1356.

D'Cruz, P.M., Yasumura, D., Weir, J., et al. (2000). Mutation of the receptor tyrosine kinase gene Mertk in the retinal dystrophic RCS rat. Hum. Mol. Genet. 9, 645–651.

Douglas, R.M., Alam, N.M., Silver, B.D., et al. (2005). Independent visual threshold measurements in the two eyes of freely moving rats and mice using a virtual-reality optokinetic system. Vis. Neurosci. 22, 677–684.

Dunnett, S.B., and Rosser, A.E. (2004). Cell therapy in Huntington's disease. Neuro. Rx 1, 394–405.

Friedman, D.S., O'Colmain, B.J., Munoz, B., et al. (2004). Prevalence of age-related macular degeneration in the United States. Arch. Ophthalmol. 122, 564–572.

Gal, A., Li, Y., Thompson, D.A., et al. (2000). Mutations in MERTK, the human orthologue of the RCS rat retinal dystrophy gene, cause retinitis pigmentosa. Nat. Genet. 26, 270–271.

Girman, S.V., Wang, S., and Lund, R.D. (2005). Time course of deterioration of rod and cone function in RCS rat and the effect of subretinal grafting; a light- and dark-adaptation study. Vis. Res. 45; 343–354.

Haruta, M., Sasai, Y., Kawasaki, H., et al. (2004). *In vitro* and *in vivo* characterization of pigment epithelial cells differentiated from primate embryonic stem cells. Invest. Ophthalmol. Vis. Sci. 45, 1020–1025.

Haruta, M. (2005). Embryonic stem cells: potential source for ocular repair. Semin. Ophthalmol. 20, 17–23.

Klimanskaya, I., Hipp, J, Rezai, J.K.A., et al. (2004). Derivation and comparative assessment of retinal pigment epithelium from human embryonic stem cells using transcriptomics. Cloning Stem Cells 6, 217–245.

Klimanskaya, I., and McMahon, J. (2004). Approaches for derivation and maintenance of human ES cells: detailed procedures and alternatives. In *Handbook of Stem Cells. Vol. 1: Embryonic Stem Cells*. R. Lanza, et al., eds. (Elsevier / Academic Press, San Diego).

Lanza R., Blau, H., Melton, D., et al. eds. (2004). *Handbook of Stem Cells* (Elsevier / Academic Press, San Diego).

LaVail, M.M. (2001). Legacy of the RCS rat: impact of a seminal study on retinal cell biology and retinal degenerative diseases. Prog. Brain Res. 131, 617–627.

LaVail, M.M., Unoki, K., Yasumura, D., et al. (1992). Multiple growth factors, cytokines, and neurotrophins rescue photoreceptors from the damaging effects of constant light. Proc. Natl. Acad. Sci. U.S.A 89, 11249–11253.

Li, N., Fan, W., Sheedlo, H.J., et al. (1996). Photoreceptor repair in response to RPE transplants in RCS rats: outer segment regeneration. Curr. Eye Res. 15, 1069–1077.

Lund, R.D., Adamson, P., Sauve, Y., et al. (2001). Subretinal transplantation of genetically modified human cell lines attenuates loss of visual function in dystrophic rats. Proc. Natl. Acad. Sci. USA 98, 9942–9947.

Lawrence, J.M., Keegan, D.J., Muir, E.M., et al. (2004). Transplantation of Schwann cell line clones secreting GDNF or BDNF into the retinas of dystrophic Royal College of Surgeons rats. Invest. Ophthalmol. Vis. Sci. 45:267–274.

Mueller, D., Shamblott, M.J., Fox, H.E., et al. (2005). Transplanted human embryonic germ cell–derived neural stem cells replace neurons and oligodendrocytes in the

forebrain of neonatal mice with excitotoxic brain damage. J. Neurosci. Res. 82, 592–608.

Pinilla, I., Lund, R.D., Lu, B., et al. (2005b). Measuring the cone contribution to the ERG b-wave to assess function and predict anatomical rescue in RCS rats. Vision Res. 45, 635–641.

Pinilla, I., Lund, R.D., and Sauve Y. (2004). Contribution of rod and cone pathways to the dark-adapted electroretinogram (ERG) b-wave following retinal degeneration in RCS rats. Vision Res. 44, 2467–2474.

Pinilla, I., Lund, R,D, and Sauve, Y. (2005a). Cone function studied with flicker electroretinogram during progressive retinal degeneration in RCS rats. Exp. Eye Res. 80, 51–59.

Prusky, G.T., Alam, N.M., Beekman, S., et al. (2004). Rapid quantification of adult and developing mouse spatial vision using a virtual optomotor system. Invest. Ophthalmol. Vis. Sci. 45, 4611–4616.

Sheedlo, H.J., Li, L., and Turner, J.E. (1991). Photoreceptor cell rescue at early and late RPE-cell transplantation periods during retinal disease in RCS dystrophic rats. J. Transplant. 2, 55–63.

Sauve, Y., Girman, S.V., Wang, S. et al. (2002). Preservation of visual responsiveness in the superior colliculus of RCS rats after retinal pigment epithelium cell transplantation. Neuroscience 114, 389–401.

Tada, A., Wada, Y., Sato, H., et al. (2006). Screening of the MERTK gene for mutations in Japanese patients with autosomal recessive retinitis pigmentosa. Mol. Vis. 12, 441–444.

Thomson, J.A., Itskovitz-Eldor, J., Shapiro, S.S., et al. (1998). Embryonic stem cell lines derived from human blastocysts. Science 282, 1145–1147.

Wang, S., Lu, B., and Lund, R.D. (2005). Morphological changes in the Royal College of Surgeons rat retina during photoreceptor degeneration and after cell-based therapy. J. Comp. Neurol. 491, 400–417.

Wang, S., Lu, B., Wood, P., et al. (2005). Grafting of ARPE-19 and Schwann cells to the subretinal space in RCS rats. Invest. Ophthalmol. Vis. Sci. 46:2552–2560.

Zhang, X., and Bok, D. (1998). Transplantation of retinal pigment epithelial cells and immune response in the subretinal space. Invest. Ophthalmol. Vis. Sci. 39, 1021–1027.

Address reprint requests to:
Dr. Robert Lanza
Advanced Cell Technology
381 Plantation St.
Worcester, MA 01605

E-mail: RLanza@advancedcell.com